Adsorption and Separation of Xylene Isomers and Ethylbenzene on Two Zn−Terephthalate Metal−Organic Frameworks

ARTICLE *in* THE JOURNAL OF PHYSICAL CHEMISTRY C · DECEMBER 2009

Impact Factor: 4.77 · DOI: 10.1021/jp9063017

5 AUTHORS, INCLUDING:

Zhi-Yuan Gu
Nanjing Normal University
24 PUBLICATIONS **2,029** CITATIONS
SEE PROFILE

Xiaoyan Cui
New York University
8 PUBLICATIONS **273** CITATIONS
SEE PROFILE

Adsorption and Separation of Xylene Isomers and Ethylbenzene on Two Zn−Terephthalate Metal−Organic Frameworks

Zhi-Yuan Gu, Dong-Qing Jiang, He-Fang Wang, Xiao-Yan Cui, and Xiu-Ping Yan*

Research Center for Analytical Sciences, College of Chemistry, Nankai University, Tianjin 300071, China

Received: July 3, 2009; Revised Manuscript Received: November 19, 2009

Metal−organic frameworks (MOFs) with metal-containing secondary building units and organic linkers have great potential for the separation of isomers. In this work, the adsorption and separation of xylene isomers and ethylbenzene (EB) on two Zn−terephthalate MOFs (MOF-5 and MOF-monoclinic) were studied by means of pulse gas chromatography, static vapor-phase adsorption, and breakthrough adsorption. The two studied Zn−terephthalate MOFs showed different selectivity and efficiency for the separation of xylene isomers and EB. On MOF-5, EB eluted first, while other isomers eluted at the same time. MOF-monoclinic showed a preferable adsorption of *p*-xylene over other isomers. The adsorption and separation of xylene isomers and EB were equilibrium-constant-controlled on MOF-5 and diffusion-dominated on MOF-monoclinic. On the basis of the measured McReynolds constants, MOF-5 was characterized as a stationary phase of nonpolarity, whereas MOF-monoclinic as a stationary phase of intermediate polarity for gas chromatography.

1. Introduction

Metal−organic frameworks (MOFs) with various metal-containing secondary building units (SBUs) and organic ligands have received great attention due to their fascinating structures[1−3] and intriguing potential applications in hydrogen storage,[4,5] gas separation,[6,7] catalysis,[8,9] chiral separation,[10,11] sensing,[12,13] and imaging.[14,15] The diversity of MOF topologies arising from the interplay between SBUs and ligands, especially ligands with different sizes and functional groups, provides various porosity and functionality via postsynthetic modification.[16−18] Variation in available pore topologies and properties is much larger for MOFs in comparison with other types of materials, offering the opportunities to screen materials for applications.[19−21]

Xylene isomers and ethylbenzene (EB) are important raw materials in industrial process; especially *p*-xylene (pX) is used on a large scale to manufacture terephthalic acid, which is the basis for the polyester (PET) industry.[22] The separation of pX from *m*-xylene (mX) and EB is one of the most challenging issues in the chemical industry because of the similarity of their boiling points. The separation can be achieved by fractional crystallization and/or adsorption on faujasite zeolite with the aid of a simulated moving-bed technique in industrial processes.[22−24] The ionic potential of the exchanged cation affects the selective adsorption of xylene isomers and EB on faujasite zeolite,[25,26] whereas the molecular sieving effect results in different diffusivities of the isomers on MFI zeolite for membrane-based pervaporation and separation.[27,28] Recently, several MOFs have been demonstrated for the adsorption and separation of xylene isomers and EB, such as MOF-5 for selective adsorption of *o*-xylene (oX) and pX,[29] MOF Zn(BDC)-(Dabco)$_{0.5}$ (BDC = 1,4-benzenedicarboxylate, Dabco = 1,4-diazabicyclo[2.2.2]octane) for the separation of oX from other isomers,[30] MIL-47 for pore-filling-dependent separation of xylene isomers and EB,[31,32] and MIL-53 for the separation of xylene isomers and EB based on the framework-breathing effect.[33,34]

Herein, we report the adsorption and separation of xylene isomers and EB on two Zn−terephthalate MOFs with different topologies, namely, MOF-5 ($[Zn_4O(terephthalate)_3]_n \cdot mDMF$)[35] and MOF-monoclinic ($[Zn_3(terephthalate)_3(H_2O)_3(DMF)_4]_n$).[36] The adsorption, diffusion, and separation of xylene isomers and EB on the MOF-5 and MOF-monoclinic were studied by means of pulse gas chromatography (GC), static vapor-phase adsorption, and breakthrough adsorption. The McReynolds constants of the Zn−terephthalate MOFs were measured to reveal the polarity of the MOFs as the stationary phase for GC.

2. Experimental Section

Preparation and Characterization of Zn−Terephthalate MOFs. MOF-5 was synthesized according to Hafizovic et al.[37] Briefly, $Zn(NO_3)_2 \cdot 6H_2O$ (600 mg, 2 mmol) and terephthalic acid (170 mg, 1 mmol) were dissolved in DMF (20 mL). The mixture was transferred to a Teflon-lined bomb, which was then sealed and placed in an oven at 120 °C for 21 h. After cooling to room temperature, the mixture was filtered to obtain the cubic colorless crystal MOF-5. The resultant MOF-5 was washed with DMF, dried at room temperature, and activated under reduced pressure at 250 °C. The prepared MOF-5 was stored under vacuum in order to avoid the collapse of frameworks due to hydrolysis.[4] The obtained MOF-5 gave a Brunauer−Emmett−Teller (BET) surface area of 773 $m^2\ g^{-1}$.

For the preparation of MOF-monoclinic, $Zn(NO_3)_2 \cdot 6H_2O$ (1200 mg, 4 mmol) and terephthalic acid (340 mg, 2 mmol) were dissolved in DMF (40 mL), then the mixture was transferred to a three-necked flask and heated at 120 °C for 6 h. The microsize crystal MOF-monoclinic was obtained by filtering the mixture after cooling to room temperature, washed with DMF, and dried under ambient conditions. The XRD pattern of the prepared MOF-monoclinic was consistent with the simulated pattern.[36] The product was stable without phase transformation under ambient conditions. After evacuation under 250 °C for 12 h, the frameworks gave a BET surface area of 225 $m^2\ g^{-1}$.

The XRD patterns of the MOFs were recorded on a D/max-2500 diffractometer (Rigaku, Japan) using Cu Kα radiation

* To whom correspondence should be addressed. Fax: (+86)22-23506075. E-mail: xpyan@nankai.edu.cn.

10.1021/jp9063017
Published on Web 12/14/2009

(λ = 1.5418 Å). The specific surface areas of the evacuated MOFs were measured on a TriStar 3000 sorptometer (Micromeritics, U.S.A.) using nitrogen adsorption at 77 K. TGA experiments were performed on a PTC-10A thermal gravimetric analyzer (Rigaku, Japan) from room temperature to 600 °C. The surface area data, XRD pattern, and TGA curves of the prepared MOF-5 and MOF-monoclinic are shown in Table S1 and Figures S1 and S2, respectively (Supporting Information).

Pulse GC Experiments. Before packing, all evacuated MOF particles were sieved to 80/100 mesh under vacuum in a box, which was pretreated with desiccant. An AISI 304 stainless steel tube (80 cm × 1 mm i.d.) was packed with ca. 350 mg of MOF particles, and then the two ends of the tube were plugged with glass wool. The MOF-5 column was activated by heating to 320 °C at a ramp rate of 2 °C min^{-1} under nitrogen and keeping at 320 °C overnight, whereas the column of MOF-monoclinic was activated by heating to 260 °C at a ramp rate of 2 °C min^{-1} under nitrogen and keeping at 260 °C overnight. The pulse GC experiments for xylene isomers and EB on the MOF-5 and MOF-monoclinic columns were carried out with a GC-14B gas chromatograph with a flame ionization detector (FID) (Shimadzu, Japan). Liquid samples of 0.05 μL were injected to the GC system, separated on the MOFs column under the controlled temperature and precolumn pressure, and detected by FID.

Intracrystalline diffusion coefficients for xylene isomers and EB in the Zn−terephthalate MOFs were measured by a chromatographic method (Supporting Information).[38−41] The trace vapor of individual xylene isomers and EB was injected in a pulse mode using a six-port valve equipped with a sample loop of 0.5 mL, then carried through the MOF-packed columns (80 cm × 1 mm) by a nitrogen stream, and finally detected by FID. The flow rate at the outlet was measured by a soap bubble flow meter and was corrected to the specific mobile phase flow rate using temperature correction and pressure gradient correction.[42] The MOF-5 column was kept at 280 °C, whereas the MOF-monoclinic column was kept at 180 °C with a carrier gas flow varying between 0.01 and 0.1 mL s^{-1}.

Static Adsorption Experiments. Vapor-phase static adsorption experiments were performed based on the procedure of liquid-phase adsorption.[33] For each experiment, each individual isomer (pX, mX, oX, or EB) with a certain volume was injected into two sealed 20 mL bottles. One of the bottles was prefilled with 5.00 mg of evacuated MOFs, and the other was empty. The adsorption equilibrium was reached at 150 °C, with a minimum duration of 30 min. Adsorbed amounts of xylene isomers and EB were calculated from the difference between equilibrium and initial concentration, which was determined by GC using a SE-30 column (30 m × 530 μm × 1.5 μm) (Zhongke Huijie Analytical Sci. & Tech. Co. Ltd., Beijing, China). Variable amounts of xylene isomers and EB added to the bottle gave different partial pressures.

Breakthrough Adsorption Experiments. The separation ability of the MOF columns was evaluated by means of breakthrough experiments for both binary component and four-component mixtures according to existing methods.[30,32,43,44] A continuous flow of xylene isomers was generated by syringe, and the isomers were vaporized at 260 °C. The vapor was carried to the inlet of the MOF column by a nitrogen stream and passed through the MOF column (80 cm × 1 mm) at 250 °C for MOF-5 and 120 °C for MOF-monoclinic. Online analysis of the eluted mixture was carried out by GC. An SE-30 column (30 m × 0.53 mm × 1.5 μm) was used for the separation of the eluted binary mixture of EB/pX, EB/mX, EB/oX, and pX/oX every minute. A β-DEX 120 column (30 m × 0.25 mm × 0.25 μm) (Supelco, Bellefonte, PA) was used for the separation of the eluted binary mixture of pX/mX every 1 min and the eluted four-component mixture every 3 min. The adsorbed amounts were calculated by integrating the breakthrough curves.[30,43] The average selectivity for binary components in breakthrough experiments was calculated according to the adsorbed amounts and partial pressure of isomers i and j according to the following equation.[32]

$$\alpha_{ij} = \left(\frac{q_i}{q_j}\right) \times \left(\frac{p_j}{p_i}\right)$$

where q_i and q_j are the adsorbed amounts of xylene isomers i and j, respectively, whereas p_i and p_j are the partial pressures (kPa) for isomers i and j, respectively.

Determination of McReynolds Constants. McReynolds constants, which reflect the retention behavior of five probe solutes (benzene, *n*-butanol, pentan-2-one, nitropropane, and pyridine), have been used traditionally to classify chromatographic stationary phases in terms of their polarity.[45,46] In this work, McReynolds constants were also measured to describe the interactions of five probe solutes with the Zn−terephthalate MOFs. The interactions related to the five selected solutes can be described as follows:[47] *X* is for benzene, which is related to weak dispersion forces and the polarizability character of the phase. *Y* represents *n*-butanol, which indicates the hydrogen-bonding ability of the phase. *Z* represents 2-pentanone, whose behavior relates to the polarizability and part of the dipolar character of the stationary phase. *U* refers to nitropropane, which is related to the electron donor, electron acceptor, and dipolar character of the phase. The *S* term, from pyridine, a strong proton acceptor and polar molecule, indicates the acidic character of the phase. Squalane was used as a standard nonpolar stationary phase, and the McReynolds constants of MOF columns were compared to that of squalane. Retention behaviors of test solutes were determined on MOF-5 at 300 °C and on MOF-monoclinic at 160 °C to prevent condensation of test solutes in the MOF columns and to make the measurements in an acceptable time.

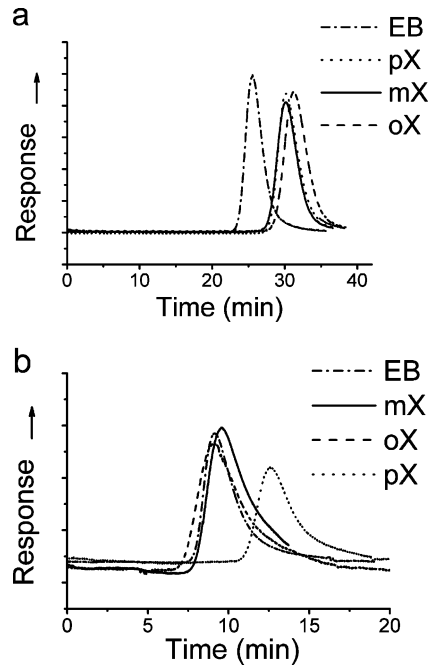

Figure 1. Chromatograms of individual xylene isomers and EB on (a) MOF-5 at 280 °C and (b) MOF-monoclinic at 180 °C.

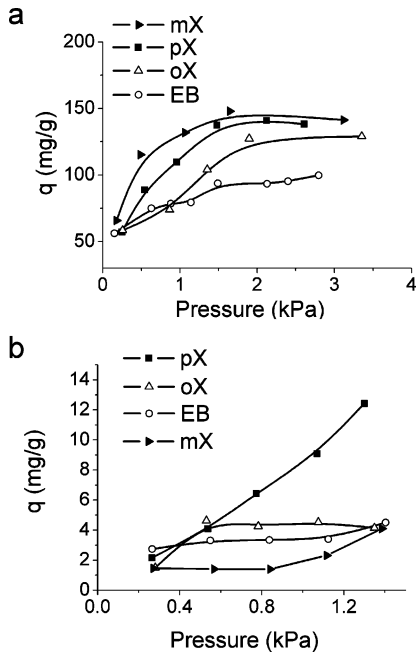

Figure 2. Static adsorption curves of xylene isomers and EB on (a) MOF-5 and (b) MOF-monoclinic at 150 °C.

3. Results and Discussion

Pulse GC experiments were carried out on the columns packed with MOF-5 and MOF-monoclinic by injecting each individual isomer. The two Zn−terephthalate MOFs showed different selectivity and efficiency for the adsorption and separation of xylene isomers and EB (Figure 1). On MOF-5, EB was clearly separated from other isomers (Figure 1a), whereas on the MOF-monoclinic column, pX was more strongly retained than other isomers (Figure 1b). The separation efficiency for each column was affected by the porosity of the MOFs. MOF-5 with a larger surface area offered a higher column efficiency (267 plates/m) than MOF-monoclinic (76 plates/m).

Static vapor-phase adsorption experiments with the isomers saturated concentrations revealed different patterns in the static adsorption of individual isomers on the Zn−terephthalate MOFs (Figure 2). On MOF-5, mX, pX, and oX were more strongly adsorbed than EB, in agreement with the elution order in pulse GC. MOF-5 showed a preferable adsorption of pX over oX in the low-pressure region (Figure 2, top), agreeing with previous observations.[29] On MOF-monoclinic, as the pressure increased, the adsorbed amount of pX significantly increased, while that of EB, mX, and oX had little changes. The different patterns in static adsorption demonstrated the selective adsorption of xylene isomers and EB on the two Zn−terephthalate MOFs under the saturation conditions.

To further investigate the selective adsorption properties of MOF-5 and MOF-monoclinic and to explore their potential application in industrial processes, binary and four-component breakthrough adsorption experiments[32,43,44] were preformed. In a binary breakthrough experiment, a vapor-phase mixture of EB and another isomer was carried through the MOF-5 column by a nitrogen stream under a constant precolumn pressure of 120 kPa (Figure 3). After an initial phase during which both isomers were fully adsorbed by MOF-5, a roll-up effect was observed: the displacement of EB by the other isomer, which was more strongly adsorbed, resulted in eluted concentrations of EB temporarily surpassing those of the feed. The average selectivity calculated from the binary breakthrough profiles on MOF-5 was 1.96 for EB/oX, 2.34 for EB/mX, and 4.14 for EB/pX. Figure 3d shows the separation of an equimolar mixture of pX, mX, oX, and EB at 250 °C. EB eluted first with good

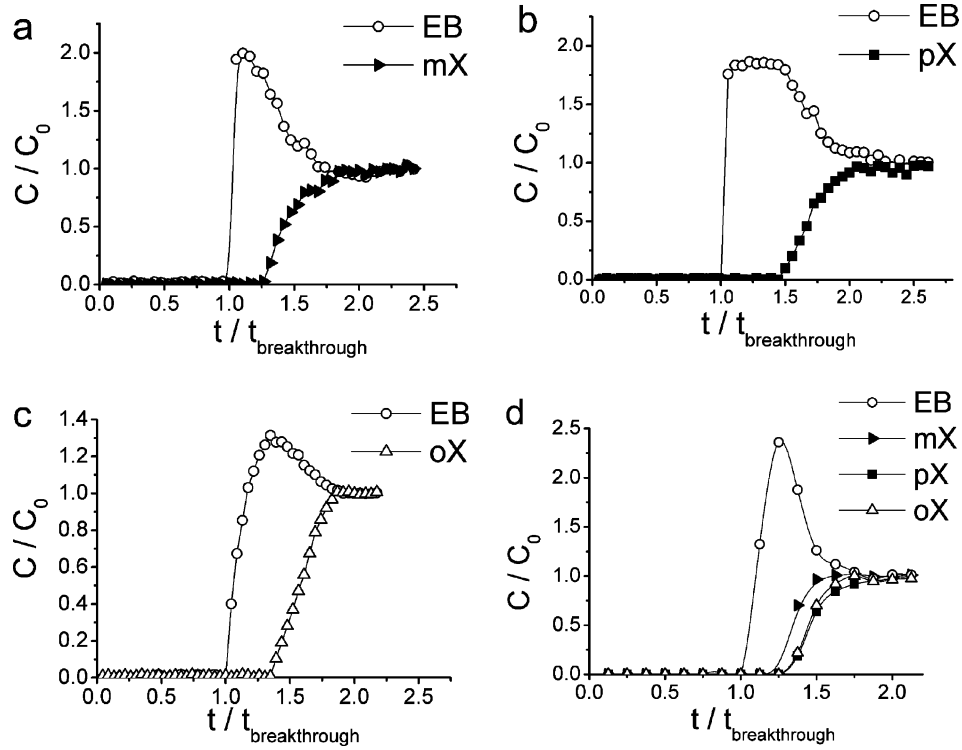

Figure 3. Breakthrough curves for the separation of equimolar binary and four-component mixtures of xylene isomers and EB on MOF-5 at 250 °C and a precolumn pressure of 120 kPa.

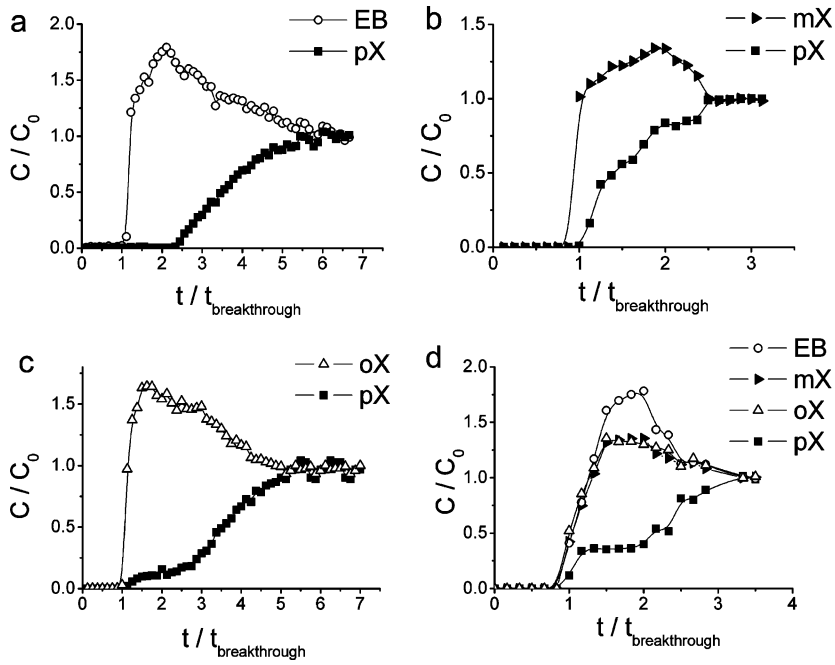

Figure 4. Breakthrough curves for the separation of equimolar binary mixtures and tetramixtures of xylene isomers and EB on MOF-monoclinic at 120 °C and 80 kPa of precolumn pressure.

TABLE 1: Equilibrium Constants (*K*) for Xylene Isomers and EB on Zn−Terephthalate MOFs

	K (mean ± 95% confidence interval)	
adsorbate	MOF-5[a]	MOF-monoclinic[b]
EB	328 ± 12	7.10 ± 0.33
mX	409 ± 10	8.13 ± 0.45
pX	431 ± 16	9.17 ± 0.07
oX	436 ± 21	9.20 ± 0.73

[a] Measured at 280 °C. [b] Measured at 180 °C.

TABLE 2: Intracrystalline Diffusion Coefficients for Xylene Isomers and EB

	diffusion coefficients (10^{-5} cm^2 s^{-1}) (mean ± 95% confidence interval)	
adsorbate	MOF-5[a]	MOF-monoclinic[b]
EB	6.0 ± 0.4	0.49 ± 0.02
pX	2.3 ± 0.1	2.00 ± 0.20
mX	4.1 ± 0.5	0.48 ± 0.01
oX	4.4 ± 1.3	0.28 ± 0.01

[a] Measured at 280 °C. [b] Measured at 180 °C.

separation from the other isomers, followed by mX, pX, and oX, which were not separated from each other under the present conditions.

Vapor-phase breakthrough experiments were also performed to demonstrate the separation potential of MOF-monoclinic for pX-containing binary mixtures (EB/pX, mX/pX, and oX/pX) and four-component mixtures (Figure 4). An analogous roll-up effect was observed on the MOF-monoclinic column. EB, mX, and oX were displaced by pX in the breakthrough processes, agreeing with the elution order in pulse GC. MOF-monoclinic gave an average selectivity of 2.52, 5.17, and 4.55 for the separation of mX/pX, EB/pX, and oX/pX binary mixtures, respectively. In a four-component breakthrough experiment, elution of all components on MOF-monoclinic started almost at the same time, but MOF-monoclinic had a preferable adsorption for pX over other isomers. The above breakthrough experiments confirmed the selective adsorption and separation of pX from other isomers on MOF-monoclinic.

Although little difference in adsorption enthalpies of xylene isomers and EB on either MOF-5 or MOF-monoclinic was observed (Table S2 in the Supporting Information), the equilibrium constants (*K*) for xylene isomers and EB were significantly different (Table 1). In accordance with the chromatographic elution order, EB with the smallest *K* value was the most weakly adsorbed isomer on each Zn−terephthalate MOF, whereas oX with the largest *K* value was the most strongly adsorbed isomer on MOF-5 and MOF-triclinic. MOF-5 is a stronger adsorbent than MOF-monoclinic for the adsorption of xylene isomers and EB. The same trend was also observed by comparing the column efficiencies.

The selectivity resulted not only from the different *K* values but also from the different sizes of pore windows in the Zn−terephthalate MOFs. The matching between the isomers and micropores in size and shape plays a crucial role in the separation and selective adsorption of isomers on MOFs[43,48] and inorganic zeolites.[27,28,49,50] The tetrahedral $[Zn_4O]^{6+}$ SBUs in MOF-5 are connected via terephthalate linkers to form pores with a cross section approximate 12 Å in size. The four isomers gave similar intracrystalline diffusion coefficients on MOF-5 (Table 2). Considering the kinetic diameters of xylene isomers and EB (5.85−6.85 Å),[50] no size hindrance was observed in the separation process on MOF-5, which was also mentioned in the sorption of alkane isomers.[51] On the other hand, the "stack" SBU in MOF-monoclinic is extended by terephthalate linkers, forming triangle pores with an edge length of ∼7 Å. pX, with the smallest kinetic diameter of 5.85 Å, gave the biggest diffusion coefficient on MOF-monoclinic (Table 2), which was also observed on MFI-type zeolite in membrane-based pervaporation and separation of xylene isomers.[27,28] The preferable adsorption of pX over oX was observed in the breakthrough experiments (Figure 4) because pX possessed a much larger diffusion coefficient and more pX could be retained on MOF-monoclinic than oX despite the similar equilibrium constants of pX and oX on MOF-monoclinic (Table 1).

TABLE 3: McReynolds Constants for Zn−Terephthalate MOF Columns

columns	X^c	Y^c	Z^c	U^c	S^c	av^c
squalane	0	0	0	0	0	0
MOF-5[a]	−101	−33	1	−28	−23	−37
MOF-monoclinic[b]	66	−23	−5	114	194	69

[a] Measured at 300 °C. [b] Measured at 160 °C. [c] *X*, *Y*, *Z*, *U*, and *S* refer to benzene, *n*-butanol, 2-pentanone, nitropropane, and pyridine, respectively. "av" is the average of the five values for each stationary phase, standing for the relative polarity of the column.[47,52]

McReynolds constants were employed to characterize the polarity of MOF-5 and MOF-monoclinic columns. Retention behaviors of five first McReynolds solutes (benzene, *n*-butanol, 2-pentanone, nitropropane, and pyridine) were determined in order to represent different interactions between probe solutes and novel stationary phases.[47,52,53] The average value of the five McReynolds constants is indicative of the polarity of a column (Table 3). McReynolds constants *X*, *Y*, *U*, and *S* of MOF-5 were even smaller than those of the reference column, squalane, which was also observed on carbon nanotubes.[53] MOF-5 could be classified as a stationary phase of nonpolar nature as it gave the smaller average value of five McReynolds constants even than a standard nonpolar phase, squalane.

The polarity of the MOF-monoclinic column is stronger than that of MOF-5 because of the larger values of *X*, *U*, and *S* on the MOF-monoclinic column. The larger value of benzene (*X*) revealed stronger retention of benzene and stronger dispersive interactions between aromatic compounds and MOF-monoclinic. In addition, larger McReynolds constants of nitropropane (*U*) and pyridine (*S*) on MOF-monoclinic showed that MOF-monoclinic had stronger proton acceptor capability and dipolar interactions than MOF-5. The three zinc atom "stack" SBU structure in MOF-monoclinic was responsible for the different retention behaviors of probe solutes. The "stack" SBUs in MOF-monoclinic that were connected by terephthalate linkers, forming a Zn−O−Zn 1-D chain and trigonal pores, showed accessibility for the isomers and resulted in stronger dipolar interactions.

4. Conclusions

In this work, we have compared MOF-5 and MOF-monoclinic for the adsorption and separation of xylene isomers and EB. Experiments of pulse GC, static vapor-phase adsorption, and breakthrough adsorption have revealed different selectivity and efficiency of MOF-5 and MOF-monoclinic for the separation of xylene isomers and EB. On MOF-5, EB eluted first, while other isomers eluted almost at the same time. MOF-monoclinic showed a preferable adsorption of pX over other isomers. The possible mechanisms have been revealed by comparing the equilibrium constants, diffusion coefficients, and polarities obtained on the two MOFs. The elution order of xylene isomers and EB on MOF-5 was controlled by the equilibrium constants. The McReynolds constants of MOF-5 demonstrated that a nonpolar phase was beneficial for a thermodynamic separation of xylene isomers and EB. The intermediate polarity of MOF-monoclinic could be attributed to the fact that the SBUs were simply more accessible for isomers. For MOF-monoclinic, the pore shape was more important. Selective adsorption of pX over other isomers on MOF-monoclinic resulted from the pore size hindrance and was dominated by the diffusion of the isomers in the micropores.

Acknowledgment. This work was supported by the National Natural Science Foundation of China (Grant No. 20935001), the National Basic Research Program of China (Grant No. 2006CB705703), and the Tianjin Natural Science Foundation (Grant No. 09JCYBJC03900).

Supporting Information Available: Surface area data, XRD patterns, and TGA curves of Zn−terephthalate MOFs and calculation of adsorption enthalpies, diffusion coefficients, and equilibrium constants of xylene isomers and EB on the Zn−terephthalate MOFs. This material is available free of charge via the Internet at http://pubs.acs.org.

References and Notes

(1) Yaghi, O. M.; O'Keeffe, M.; Ockwig, N. W.; Chae, H. K.; Eddaoudi, M.; Kim, J. *Nature* **2003**, *423*, 705.
(2) Kitagawa, S.; Kitaura, R.; Noro, S. *Angew. Chem., Int. Ed.* **2004**, *43*, 2334.
(3) Férey, G. *Chem. Soc. Rev.* **2008**, *37*, 191.
(4) Kaye, S. S.; Dailly, A.; Yaghi, O. M.; Long, J. R. *J. Am. Chem. Soc.* **2007**, *129*, 14176.
(5) Vitillo, J. G.; Regli, L.; Chavan, S.; Ricchiardi, G.; Spoto, G.; Dietzel, P. D. C.; Bordiga, S.; Zecchina, A. *J. Am. Chem. Soc.* **2008**, *130*, 8386.
(6) Yoon, J. W.; Jhung, S. H.; Hwang, Y. K.; Humphrey, S. M.; Wood, P. T.; Chang, J. S. *Adv. Mater.* **2007**, *19*, 1830.
(7) Bastin, L.; Bárcia, P. S.; Hurtado, E. J.; Silva, J. A. C.; Rodrigues, A. E.; Chen, B. *J. Phys. Chem. C* **2008**, *112*, 1575.
(8) Wu, C. D.; Lin, W. B. *Angew. Chem., Int. Ed.* **2007**, *46*, 1075.
(9) Alkordi, M. H.; Liu, Y.; Larsen, R. W.; Eubank, J. F.; Eddaoudi, M. *J. Am. Chem. Soc.* **2008**, *130*, 12639.
(10) Kesanli, B.; Lin, W. B. *Coord. Chem. Rev.* **2003**, *246*, 305.
(11) Lin, W. B. *J. Solid State Chem.* **2005**, *178*, 2486.
(12) Chen, B.; Wang, L.; Zapata, F.; Qian, G.; Lobkovsky, E. B. *J. Am. Chem. Soc.* **2008**, *130*, 6718.
(13) Lan, A.; Li, K.; Wu, H.; Olson, D. H.; Emge, T. J.; Ki, W.; Hong, M.; Li, J. *Angew. Chem., Int. Ed.* **2009**, *48*, 2334.
(14) Taylor, K. M. L.; Rieter, W. J.; Lin, W. *J. Am. Chem. Soc.* **2008**, *130*, 14358.
(15) Taylor, K. M. L.; Jin, A.; Lin, W. *Angew. Chem., Int. Ed.* **2008**, *47*, 7722.
(16) Tanabe, K. K.; Wang, Z.; Cohen, S. M. *J. Am. Chem. Soc.* **2008**, *130*, 8508.
(17) Banerjee, M.; Das, S.; Yoon, M.; Choi, H. J.; Hyun, M. H.; Park, S. M.; Seo, G.; Kim, K. *J. Am. Chem. Soc.* **2009**, *131*, 7524.
(18) Wang, Z.; Cohen, S. M. *Chem. Soc. Rev.* **2009**, *38*, 1315.
(19) Jansen, M.; Schön, J. C. *Angew. Chem., Int. Ed.* **2006**, *45*, 3406.
(20) Eddaoudi, M.; Moler, D. B.; Li, H. L.; Chen, B. L.; Reineke, T. M.; O'Keeffe, M.; Yaghi, O. M. *Acc. Chem. Res.* **2001**, *34*, 319.
(21) Eddaoudi, M.; Kim, J.; Rosi, N.; Vodak, D.; Wachter, J.; O'Keeffe, M.; Yaghi, O. M. *Science* **2002**, *295*, 469.
(22) Minceva, M.; Rodrigues, A. E. *AIChE J.* **2007**, *53*, 138.
(23) Mohameed, H. A.; Jdayil, B. A.; Takrouri, K. *Chem. Eng. Process.* **2007**, *46*, 25.
(24) Cottier, V.; Bellat, J.-P.; Simonot-Grange, M.-H.; Methivier, A. *J. Phys. Chem. B* **1997**, *101*, 4798.
(25) Kulprathipanja, S.; Johnson, J. A. *Handb. Porous Solids* **2002**, 2568.
(26) Iwayama, K.; Suzuki, M. *Stud. Surf. Sci. Catal.* **1994**, *83*, 243.
(27) Sakai, H.; Tomita, T.; Takahashi, T. *Sep. Purif. Technol.* **2001**, *25*, 297.
(28) Yuan, W.; Lin, Y. S.; Yang, W. *J. Am. Chem. Soc.* **2004**, *126*, 4776.
(29) Huang, L. M.; Wang, H. T.; Chen, J. X.; Wang, Z. B.; Sun, J. Y.; Zhao, D. Y.; Yan, Y. S. *Microporous Mesoporous Mater.* **2003**, *58*, 105.
(30) Nicolau, M. P. M.; Bárcia, P. S.; Gallegos, J. M.; Silva, J. A. C.; Rodrigues, A. E.; Chen, B. *J. Phys. Chem. C* **2009**, *113*, 13173.
(31) Alaerts, L.; Kirschhock, C. E. A.; Maes, M.; van der Veen, M. A.; Finsy, V.; Depla, A.; Martens, J. A.; Baron, G. V.; Jacobs, P. A.; Denayer, J. E. M.; De Vos, D. E. *Angew. Chem., Int. Ed.* **2007**, *46*, 4293.
(32) Finsy, V.; Verelst, H.; Alaerts, L.; De Vos, D.; Jacobs, P. A.; Baron, G. V.; Denayer, J. F. M. *J. Am. Chem. Soc.* **2008**, *130*, 7110.
(33) Alaerts, L.; Maes, M.; Giebeler, L.; Jacobs, P. A.; Martens, J. A.; Denayer, J. F. M.; Kirschhock, C. E. A.; De Vos, D. E. *J. Am. Chem. Soc.* **2008**, *130*, 14170.
(34) Finsy, V.; Kirschhock, C. E. A.; Vedts, G.; Maes, M.; Alaerts, L.; Vos, D. E. D.; Baron, G. V.; Denayer, J. F. M. *Chem.—Eur. J.* **2009**, *15*, 7724.
(35) Li, H.; Eddaoudi, M.; O'Keeffe, M.; Yaghi, O. M. *Nature* **1999**, *402*, 276.

(36) Edgar, M.; Mitchell, R.; Slawin, A. M. Z.; Lightfoot, P.; Wright, P. A. *Chem.—Eur. J.* **2001**, *7*, 5168.

(37) Hafizovic, J.; Bjorgen, M.; Olsbye, U.; Dietzel, P. D. C.; Bordiga, S.; Prestipino, C.; Lamberti, C.; Lillerud, K. P. *J. Am. Chem. Soc.* **2007**, *129*, 3612.

(38) Haq, N.; Ruthven, D. M. *J. Colloid Interface Sci.* **1986**, *112*, 164.

(39) Haq, N.; Ruthven, D. M. *J. Colloid Interface Sci.* **1986**, *112*, 154.

(40) Armatas, G. S.; Petrakis, D. E.; Pomonis, P. J. *J. Chromatogr., A* **2005**, *1074*, 53.

(41) Zhang, J.; Zhao, Z.; Duan, A.; Jiang, G.; Liu, J.; Zhang, D. *Energy Fuels* **2009**, *23*, 617.

(42) Gray, D. G.; Guillet, J. E. *Macromolecules* **1973**, *6*, 223.

(43) Bárcia, P. S.; Zapata, F.; Silva, J. A. C.; Rodrigues, A. E.; Chen, B. *J. Phys. Chem. B* **2007**, *111*, 6101.

(44) Britt, D.; Tranchemontagne, D.; Yaghi, O. M. *Proc. Natl. Acad. Sci. U.S.A.* **2008**, *105*, 11623.

(45) McReynolds, W. O. *J. Chromatogr. Sci.* **1970**, *8*, 685.

(46) Grob, R. L., Barry, E. F., Eds. *Modern Practice of Gas Chromatography*, 4th ed.; John Wiley & Sons, Inc.: Hoboken, NJ, 2004.

(47) Berthod, A.; Zhou, E. Y.; Le, K.; Armstrong, D. W. *Anal. Chem.* **1995**, *67*, 849.

(48) Chen, B.; Liang, C.; Yang, J.; Contreras, D. S.; Clancy, Y. L.; Lobkovsky, E. B.; Yaghi, O. M.; Dai, S. *Angew. Chem., Int. Ed.* **2006**, *45*, 1390.

(49) Keizer, K.; Burggraaf, A. J.; Vroon, Z. A. E. P.; Verweij, H. *J. Membr. Sci.* **1998**, *147*, 159.

(50) Gump, C. J.; Tuan, V. A.; Noble, R. D.; Falconer, J. L. *Ind. Eng. Chem. Res.* **2001**, *40*, 565.

(51) Zhang, L.; Wang, Q.; Wu, T.; Liu, Y. C. *Chem.—Eur. J.* **2007**, *13*, 6387.

(52) Armstrong, D. W.; He, L. F.; Liu, Y. S. *Anal. Chem.* **1999**, *71*, 3873.

(53) Karwa, M.; Mitra, S. *Anal. Chem.* **2006**, *78*, 2064.

JP9063017